

Physicochemical Properties of Synthesized Organobentonite

A. Ben Othman, F. Ayari, S. Mezguich and M. Trabelsi-Ayadi

Laboratory of Applications of Chemistry for Resources and Natural Substances and the Environment. (LACReSNE) Faculté des sciences de Bizerte Zarzouna 7021 Bizerte Tunis, Université de Carthage

Abstract--Surfactant modified bentonite was prepared using HDTMA-Br at 0.5CEC and 1CEC, obtained organobentonite labeled AB-p0.5T and AB-p1T were characterized by several methods such as Infrared spectroscopy (IR), (BET) and Scanning electron microscope (SEM). These methods were used to provide new visions into the interlayer structure of organoclays and to determine their physicochemical properties. IR spectroscopy showed the existence of HDTMA functional groups on bentonite surface. The BET surface area significantly decreased after modification due to the coverage of the pores sites into AB-p.

Acid-base potentiometric titration and mass titration behavior of all samples were investigated. The point of zero charge (PZC) estimated by these both methods was about 6.4 for AB-p and 7.8 and 8.2 for AB-p0.5T, and AB-p1T respectively. Bentonite which has hydrophilic property in nature converts to hydrophobic after organophilisation. Hybrid material develops more positives surface charges with hydrophobic character and great basal spacing layer; therefore these materials can be very useful in industry applications and as adsorbent materials to remove anionic pollutants from wastewater.

Keywords—Organobentonite; caracterisation; HDTMA

I. INTRODUCTION

Surface properties of natural bentonite can be significantly modified with great organic surfactants such as long chain quaternary alkylammonium salts by simple ion-exchange reactions, assured by van der Waals interaction between organic surfactant cations and the adsorbate [1,2]. Intercalation of cationic surfactant not only changes the surface properties from hydrophilic to hydrophobic, but also greatly increases the basal spacing of the layers.

Organobentonite becomes more effective adsorbent; In particular the hydrophobic nature of the organoclay suggests the material can be used as a filter material for water purification from organic pollutants [3], as the transport of nonionic contaminants in ground water [4] as rheological control agents [5] and electric materials [6]. Diverse sorption mechanisms are proved, strongly depending on the molecule structure of the organic pollutants and quaternary ammonium cations used to modify clay. The adsorption behavior of organoclays prepared by different types of surfactant (small or large organic cations) creates diverse adsorption mechanisms and it touches considerably the adsorption capacity of organoclays [7]. The charge density of the clay layer is responsible for the arrangement of intercalated organic

cations within the interlayer of clay which controls the adsorption capacity of organoclays.

II. MATERIALS AND METHODS

Preparation of collected clay sample from Ain-Berda (Bizerte, North-East of Tunisia) included air drying, crushing by mortar and pestle and passing through a 60-mesh sieve. The clay fine fraction (particle size < 2 μm) was purified by the classic method, by several cycle exchanged with NaCl solution (1mol L^{-1}) under stirring during 24 h for five times to form the sodium-saturated clay sample. Na-saturated clay was washed with distilled water until chloride free as confirmed by the AgNO_3 test. Obtained sample denoted (AB-p) was dried at 80°C and grounding.

Characterization clay sample included surface area measurement, mineralogical analysis. Chemical analyses were obtained by using X-ray diffraction studies (Philips goniometer, PW1730/10, using the $K\alpha$ radiation of copper). Infrared spectra obtained by using KBr pellets were recorded with a Perkin Elmer 783 dispersive spectrometer from 4000 to 400cm^{-1} . Cation exchange capacities (CEC) were estimated by the MANTIN method. Thermal analysis was also studied.

Sample morphology was recognized by Transmission electron microscopy (TEM). BET surface area (S_{BET}) and pore volumes of clay sample were measured using the physical adsorption of nitrogen by Quantachrome Autosorb-1 instrument. The adsorption of methylene blue dye on bentonite in solutions is used to determine either their cation-exchange capacities (CEC) or their total specific surface area (S_s) via Uv-spectrometer.

III. RESULTATS AND DISCUSSION

A. X-ray diffraction

As shown in Figure I. Quartz (reflection at 3.34\AA and 4.27\AA) and calcite (reflection at 3.03\AA) are the major impurities. The positions of 001 reflections of the smectite appear at 14.25\AA for the sample, suggesting that the fraction might be in the Ca-exchange form. The purified sample with Na-exchange shows the position of the 001 reflection at $d_{001}=12.30\text{\AA}$, characteristic of a sodium smectite or an interstratified sample of these minerals with illite.

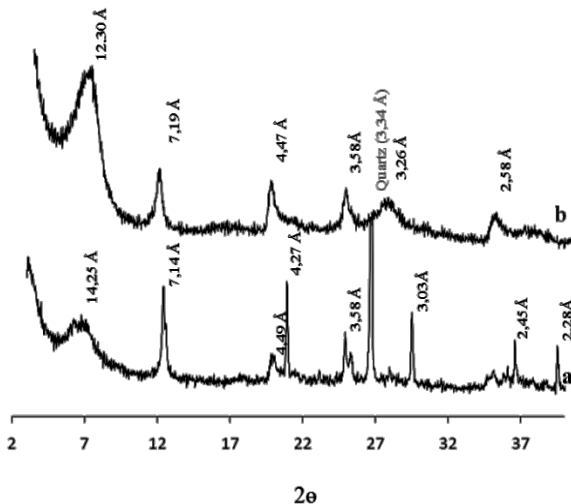


Fig.I X-ray diffractograms of crude (a) and purified (b) clay.

B. Infrared spectra

Infrared spectra (Fig.II) are evident in the frequency range of 4000–400 cm⁻¹. The most significant adsorption bands were discerned and identified by means of previous work in literatures.

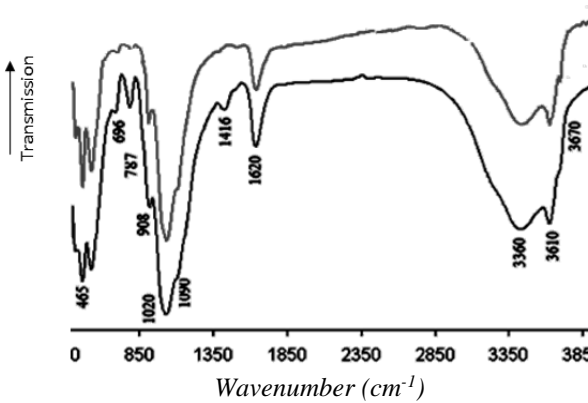


Fig.II: Infrared spectra of crude and purified sample

Infrared spectra of samples AB-r and AB-p are given in Figure II.

These show mainly the bands illustrated as follows:
 Band that lies between 1600-1700cm⁻¹ relate to the OH⁻ deformation of water (H-O-H bending), suggests the presence of adsorbed water. The band that appears between 3200 -3800cm⁻¹ is typical for bentonite with large amounts of Al in the octahedral sheet, attributed to H–O–H stretching vibration of adsorbed water.
 Si-O group is characterized by an intense band between 900-1200cm⁻¹, centered around 1020cm⁻¹ corresponding to stretching vibrations of Si-O. Bands observed at 787cm⁻¹ was due to stretching vibrations of Si-O-Al group.

C. CEC measurement and Specific surface area

Fixing cations is due to the existence of a negative structural charge of the clay.
 The results obtained by the Mantin method as described in previous work [8] for CEC determination are given in Table I. Specific surface area show that the CEC increases

after purification and it corresponds to that of a smectite group. In fact the values obtained belong to the CEC interval of a smectite (CEC between 80 and 150 meq / 100g).

Table I: CEC and Ss of AB-r et AB-p

Sample	Crude clay	Pure clay
Ss (m ² g ⁻¹)	336.27	531.2
CEC(meq/100g hyd. clay)	50.86	76.16

D. Potentiometric titration

The evolution of the surface charge density at different ionic strengths (0.01M, 0.1M and 0.5M) in function of pH for the clay slurry AB-p is given in Figure III. Curve is composed of two branches one positive and the other negative. This allows us to distinguish two types of reaction sites on the surface: the protonation sites for pH <6 and deprotonation sites for pH > 6. Surface charge decreases when the pH increases indicating that the number of sites positively charged reduced in favor of negatively charged sites. The increase in ionic strength causes an increase in the surface charge due to an increase in shielding loads thus limiting the electrostatic repulsions between neighboring sites and to increase the rate of protonation or deprotonation of the surface sites.

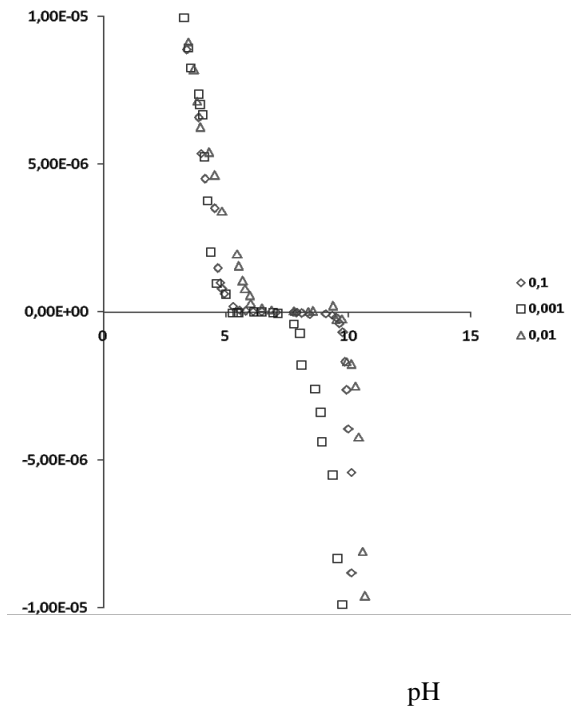


Fig.III: Variation of surface charge density (I = 0.01M, 0.1M and 0.5M) in function of pH for the clay slurry AB-p

E. Specific charge density σ

The specific charge density is the ratio of cation exchange capacity CEC vs surface area Ss of the clay particle:

$$\sigma \text{ (mmol.m}^{-2}\text{)} = \text{CEC} / \text{Ss}$$

Results show that σ (AB-r) = 0.104 mmol/m² and σ (AB-p) = 0.121 mmol/m². Data of the specific charge density (σ) of the raw and purified sample have a lower value (σ < 1mmol.m⁻²) suggest that this clay is swelling [9].

F. Thermal analysis

Differential thermal analysis and thermogravimetric analysis (DTA/TGA) DTA and TGA were merely used as complementary methods with respect to the other techniques. The interpretation [1,10,11] of the DTA-TGA curves of the raw and purified samples leads to the following results (Figure IV: a, b):

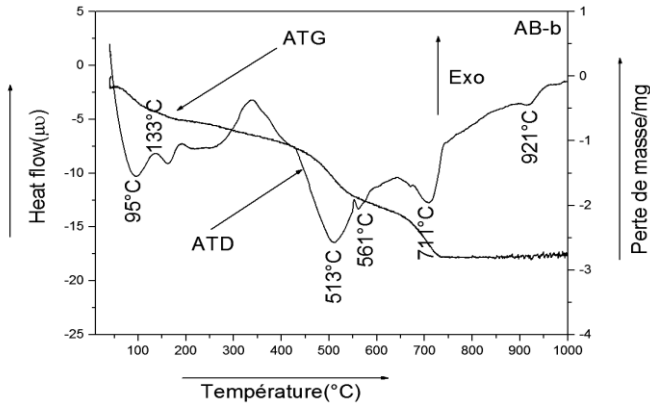


Fig. V, a: ATD-ATG of AB-r

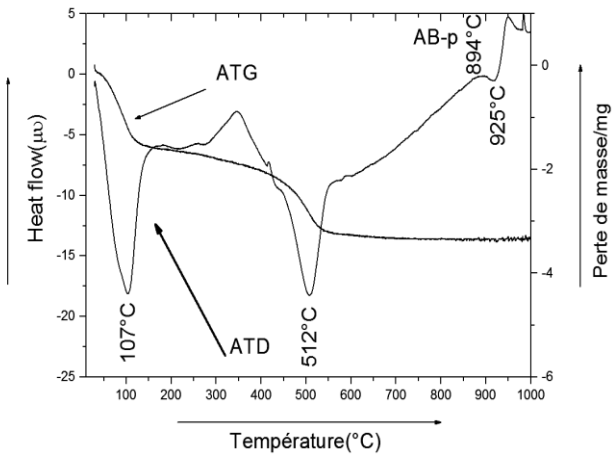


Fig.IV, b: ATD-ATG of AB-p

Thermogram ATD of the raw sample AB-r (Figure IV, a) shows two peaks between 95 and 133°C; these transformation are due to the removal of adsorbed and interlayer water from the clay mineral. A high intensity endothermic peak at 513°C which corresponds to the loss of hydroxyl groups from the clay mineral structure (clay dehydroxylation). This probably indicates the presence of a beidellitique character or presence of illite-smectite interstratification. The peak at 561°C relates to the transformation of the α quartz β quartz. The thermogram of the sample purified AB-p (Figure IV, b) shows an endothermic peak at 107°C with loss of interlayer water and a peak at 512°C relative to the dehydroxylation of the purified clay.

The curves of thermogravimetric (TGA) analyze to track the loss of mass of the sample. These curves represent three mass losses for the raw clay and two losses for purified clay. The first mass loss is between 100 and 130°C, corresponding to the loss of moisture and water interlayer. The second mass loss to 513°C and 512°C, corresponding to the loss of water content. The third mass loss occurs at

561°C and corresponds to the decarbonisation of clay. This loss appears only on the thermograms of raw clay AB-r. Loss percentages waters constitution and hydration are illustrated in the following Table II:

Table II (%) Loss of water

Sample	hydratation loss	constitution loss
AB-r	2,24	4,097
AB-p	6,522	5,261

F. Preparation of HDTMA organoclays (in olution)

Syntheses of surfactant-modified bentonite were performed by mixing an amount of Na-bent, initially dispersed in ~100mL of deionized water, with a stoichiometric amount of surfactant (0.5CEC and 1CEC) dispersed in 200mL of deionized water, added slowly to the clay suspension, Surfactant used in this study is precisely hexadecyltrimethylammonium bromide (HDTMABr) (Fig.V). Reaction mixtures were stirred for 12 h at 80°C. After maturation, centrifugation, and several successive dialyses, the prepared organoclay materials were washed with distilled water to remove any excess surfactants, until free of bromide anions (tested by $AgNO_3$), dried at 80°C, ground in an agate mortar and passed through a 200 mesh sieve

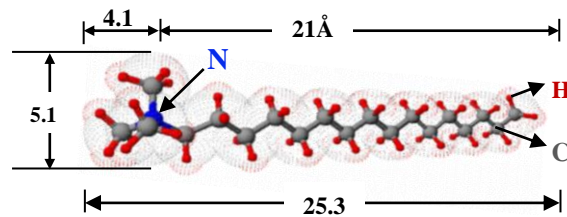


Fig.V: Chemical structure of HDTMA

Organoclay prepared at a surfactant concentration of 0.5CEC was marked as AB-p0.5T and the other was marked as AB-p1T.

G. Characterization of HDTMA organoclays material

G.1. FTIR analysis

The infrared spectra were recorded with Perkin Elmer 783 dispersion spectrometer in the range of 4000 to 400 cm^{-1} . FTIR spectroscopy has been employed in this investigation to pinpoint the most significant modification by means of HDTMA grafting in the AB-p.

As can be seen from Figure VII and on the basis of information given by earlier works [12-13] absorption bands at 3626 cm^{-1} and 3622 in AB-p and organoclays respectively are owing to hydroxyl group vibration in Mg-OH-Al, Al-OH-Al and Fe-OH-Al elements in the octahedral layer [14].

Accordingly to literature, the position and shape of the -OH stretching band in the FT-IR spectra of bentonite minerals is basically influenced by the nature of the octahedral atoms to which the hydroxyl groups are coordinated. Thus absorption band at 3626 cm^{-1} , found in

the spectrum of AB-p, is typical for bentonite with large amounts of Al in the octahedral sheet.

Broad bands at around 3430 in both AB-p and organoclays were attributed to H-O-H stretching vibration of adsorbed water.

When the concentration of surfactant was higher than 100% CEC appearance of peak at around 3017 cm^{-1} (stretching peak of the N-H groups) was noted; the intensity of this peak increase with surfactant concentration and is a suggestion for the change of bentonite with surfactant (HDTMA-Br) functional groups.

Peaks at around 1623 (AB-p) relate to the OH-deformation of water (H-O-H bending), suggests the presence of adsorbed water. These bands appear in both AB-p and the hybrid synthesized organoclay (AB-p0.5T and AB-p1T), yet its position is gradually shifted from 1628 cm^{-1} (for sample AB-p0.5T) to 1649 cm^{-1} (for sample AB-p1T) with increases of surfactant concentration this reflects that the amount of hydrogen bonded water molecules present in the organoclays with higher concentration of surfactant is less than those with lower concentration of surfactant. This could be explained by that the H₂O content is reduced with the replacement of the hydrated cations by HDTMA⁺ ions in the interlayer space. Therefore internal surface property of bentonite was converted from hydrophilic to hydrophobic. In addition, comparing to HDTMA spectra, infrared spectrum of organoclays showed a pair of a strong vibrations at around 2921 and 2854 cm^{-1} attributed to symmetric and asymmetric stretching vibrations of methylene groups (νCH_2), which are absent in AB-p, this attest transformation of Na-benton organoclay with the surfactant cation (HDTMA⁺). It was noted that the frequency and the intensity of these broad bands changed with the amount of intercalated surfactant. These frequencies are extremely sensitive to the conformational ordering of the chain of cationic surfactant onto clay [15].

Existence of two peaks at around 1435 and 1473 cm^{-1} (which are absent in AB-p) specifying the presence of C-N vibrations in tertiary amines. With a large addition of HDTMA, the spectra were similar to those of solid HDTMA because the chains were densely packed; this observation clearly indicates that the surface modification of Na-clay is achieved by surfactant.

Adsorption band at around 720 cm^{-1} correspond to the methylene rocking mode ($\rho(\text{CH}_2)$), independent of chain conformation, this mode is split due to interchain interaction between contiguous CH₂ groups of adjoining chains

The bands at around 1110 and 1030 cm^{-1} , represent the Si-O coordination vibrations and the stretching of Si-O in the Si-O-Si groups of the tetrahedral sheet, respectively. Also, Si-O-Al (octahedral) and Si-O-Si bending vibrations were observed at 520 and 470 cm^{-1} , respectively, for both AB-p and organo-bentonite, as in other silica and silicate systems.

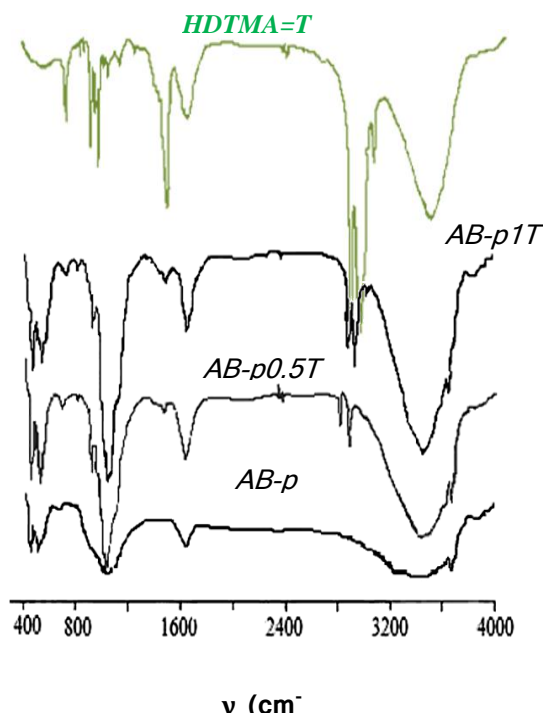
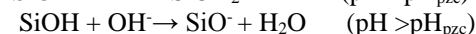
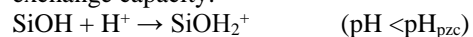


Fig. VI: FTIR of AB-p, HDTMA solid and HDTMA pillared bentonite

G.2. Surface charge density σ_H and pH of point of zero charge pH_{PZC}

Bentonite clay minerals are characterized by a non-neutral electric surface. There are two types of load: (i) a structural charge (continued charge), related to ionic substitutions (Al^{3+} for Si^{4+} in the tetrahedral site, Mg^{2+} or Fe^{2+} for Al^{3+} in the octahedral site), of negative sign, (ii) a surface charge related to the hydrolysis of broken bonds Si-OH and Al-OH along surfaces (in edge of layer). At lower pH, clay is characterized by anionic exchange capacity: H^+ binds more compared to OH^- , a positive load develops. At high pH, a cationic exchange capacity (CEC) develops: The OH^- bind more compared to H^+ and negative charge develops.

The hydrolysis of Si-OH or Al-OH bonds along the clay lattices produces the surface charge. Depending on the silica structure and the pH of the solution, the net surface charge can be either positive or negative. At pH less than pH_{PZC} , the clay would have an anion exchange capacity, while at pH higher than pH_{PZC} , the clay would have a cation exchange capacity:



pH_{PZC} is the pH where the net charge of the hydroxide surface is zero, provided there is no specific adsorption of the electrolyte ions. Under these conditions the PZC is coincident with the isoelectric point (IEP) which is defined as the pH where electrophoretic mobilities or other electrokinetic properties become zero.

The replacement of the interlayer exchangeable cations with organoammonium ions results in changes in the surface properties and the modified silicates have found application in the fields of construction of novel host-guest systems where hydrophilic silicates do not have access. When bentonites are used as adsorbents, organic modification is often used to modify the chemical nature of the interlayer space to create the adsorbent for target adsorbates.

Surface of organobentonite was charged when the organobentonite was placed in a water solution. The surface charge was caused by the interaction between the ion in the solution and the functional groups of organobentonite surface. Normally, the surface charge of a solid is dependent on the type of ion present in the solution, the characteristic of the surface, the nature of the adsorbent and the solution pH.

The pH_{PZC} of purified and organo-modified samples were estimated by the masse titration and potentiometric methods.

G.2.1 Masse titration

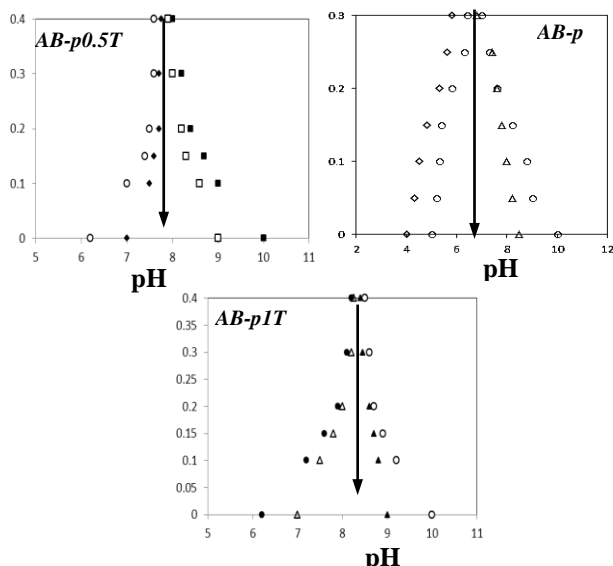


Fig.VII: Mass titration curves of AB-p and organobentonite obtained at $I=0.1M$ of KCl and at different pH values

Mass titration data performed at 0.1M KCl concentrations are presented in fig. IX. The pH gradually changes with addition of solid and asymptotically approaches a limiting value. The direction of the pH variation depends on the pH of the starting KCl solution. Therefore, the pH where solid addition does not produce any change in the pH of the initial KCl solution can be estimated by interpolation. The point of zero charge (PZC) estimated are marked with arrows in the figure IX, their values were 6.2, 7.8 and 8.2 for AB-p, AB-p0.5T and AB-p1T adsorbents respectively. It is imperative to note that the PZC of organobentonites was displaced to the basic zone compared to that of the pure bentonite. The shift of PZC is about 3units of pH, it increases from 6.2 to 8.9. These news synthesized materials develop more positive charge then untreated sample (AB-p) so more possibility to remove anionic compounds from wastewater.

G.2.2 Potentiometric titration

To better understand surface properties, potentiometric titrations were conducted to measure the proton adsorption or proton charge and determine the point of zero charge PZC. The results of the surface proton density σ_H vs pH of the purified clay and organoclays dispersed in 0.1M KCl are shown in fig VIII. Data from potentiometric titration suggest two dominant sorption reactions: cation exchange at permanently negative charged sites on the siloxane faces including interlayer regions of bentonite, with the interlayer region accounting for the relatively slow sorption, and inner-sphere surface complex formation at variable charge surface hydroxyl groups at the crystal edges. At the acidic pH range, the degree of protonation increased with increasing surfactant in the interlayer and the opposite was observed in the alkaline pH range. The organobentonites have a surface charge density produced by protonation and deprotonation of inner-sphere surfactant-hydroxyl surface complex formed at variable-charge hydroxyl groups at the edges.

PZC of the organobentonites moved to the basic pH according to the HDTMA⁺ intercalation degree (fig. VIII). The PZC results were summarized in table III which shows that the shift of PZC is about three units of pH, it increase from 6.7 (AB-p) to 8.2 (AB-p1T).

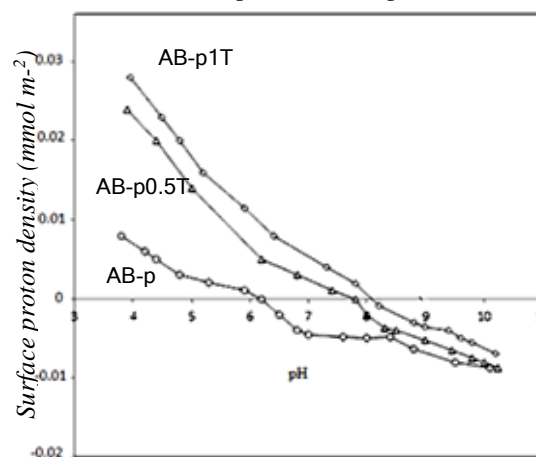


Fig.VIII: Potentiometric titration curves of AB-p and organobentonite obtained at $I=0.1M$ of KCl.

Very good agreement between both kinds of experiments; mass titration and potentiometric titration can be enhanced.

The loading of surfactants causes a transformation of clay surface property from hydrophilic to hydrophobic. Hydrophobicity suppressed the formation of bound HO layers on the surface.

H. Scanning electron microscope (SEM)

SEM photomicrographs obtained for Na-bent and organo sample (AB-p1T) are illustrated in fig. IX. Surface of AB-p looks very smooth with fluffy appearance and curved plates. After cationic surfactant insertion reaction significant changes were observed. Surface morphology loses its foliated structure and became rougher with many small and aggregated particles and the plates become relatively flat, this is probably occurred due to the

reduction in certain crystalline domains of the clay particles with the increase of surfactant packing density in the interlayer, the curved plates in AB-p will change to flat layers.

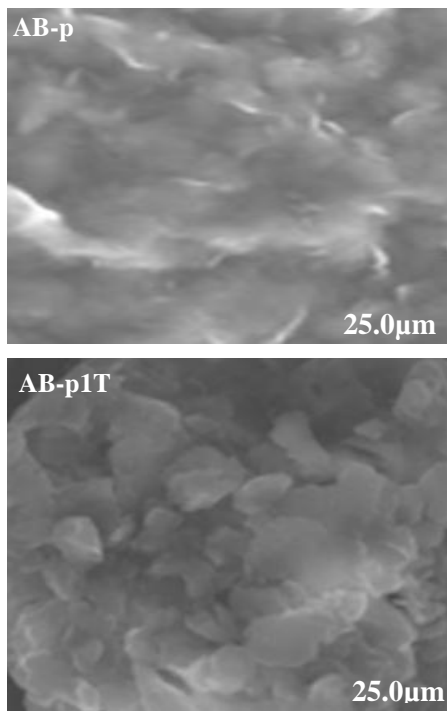


Fig. IX: SEM images of AB-p and organobentonite

I. Specific surface area S_{BET} and cation exchange capacity (CEC)

Specific surface area (figures not shown), pore volume, and CEC of the AB-p and hybrid organoclays are presented in table IV.

Surface area drops dramatically from AB-p ($68.28\text{cm}^3\text{g}^{-1}$) to AB-p1T ($3.82\text{cm}^3\text{g}^{-1}$). It is also found that the pore volume for organoclays decreases with an increase of loaded surfactants. This is due to the fact that interparticle pores of bentonite are covered and the interlamellar spaces are blocked, lead to inhibition of the passage of N_2 molecules. This is distinctive by the decrease of pores volumes by HDTMA increasing density. Micropores surface area ($S_{\mu p}$) and micropores volumes ($S_{\mu p}$) were annulled after the organophilic modification.

Table IV. Textural parameters and CEC studied of AB-p and AB-pxT

samples	S_{BET} (m^2g^{-1})	$S_{\mu p}$ (m^2g^{-1})	V_p (cm^3g^{-1})	CEC (meq/100g)
AB-p	68.28	8.7	0.138	78
AB-p0.5T	19	-	0.11	48
AB-p1T	3.82	-	0.008	36

The cation exchange capacity (CEC) of AB-p and hybrid organoclays, determined by using Mantin method [12] were estimated.

CEC decreases with the increase of HDTMA density, it shifts from 78 (AB-p) to 36meq/100g (AB-p1T). These results confirm those of acid-base potentiometric titration. The PZC of the organobentonite was basic (table IV) because the adsorption of the surfactant modified the

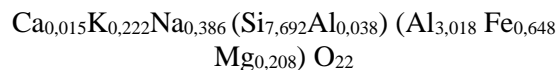
surface character. The increase of pH_{PZC} after surfactant treatment indicates that the organoclay becomes more positive and the surface properties of the adsorbent change from hydrophilic to hydrophobic by the intercalation of the alkylammonium molecule. Then, intercalations of organic molecules generate higher adsorption capacity for organic molecules [16-17].

From CEC and S_{BET} results the surfactant cations mainly occupy both the clay interlayer space and the interparticle pores in the organoclays prepared at high surfactant concentrations. It can be estimative that HDTMA^+ occupies interlayer space, via cation exchange with Na^+ interlayer, and the surface adsorption sites.

IV. CONCLUSION

Clay mineral collected from Bizerte Tunisia (Ain-Berda) is a phyllosilicate of 2:1 type. Results reveal that it has a swelling nature and belong to smectite group family. It is calcium smectic in nature associated to a small amount of kaolinite. The percentage of estimated smectic fraction is 78%.

Chemical formula has been estimated as:



After organomodification the clay sample became hydrophobic with high positive charge density, lower CEC and S_{BET} . Organobentonite appear very useful for anionic molecules adsorption which is difficult with natural benonite.

REFERENCES

- [1] Y. H. Shen., *Chemosphere* 44 (2001) 989.
- [2] A. S.Ozcan, B. Erdem...A. Ozcan., *J. Colloid Interface Sci.* 44 (2004) 280.
- [3] L.Z Zhu, Y.H. Su.,... *Clays and Clay Miner.* 49 (2002) 421-427.
- [4] M.Yurdakoc; Akc May; Y. Tonbul.; Ok. K. F. Yurdakoc; *Microporous Mesoporous Mater.* 111(2008) 211
- [5] E. Manias, G. Hadziioannou, G. Brinke., *Langmuir* 12(2003) 4587-4593.
- [6] J.H. Wu., M.M. Lerner., *Chem. Mater.* 5(1993) 835-838.
- [7] S. Xu., G. Sheng., S.A. Boyd., *Adv. Agron.*59(1997) 25-62.
- [8] P. C LeBaron, Z. Wang, T. J Pinnavaia. *Polymer-layered silicate nanocomposites: an overview.* *Applied Clay Science* (1999), 15, 11-29.
- [9] M. Knite., V. Teteris., A. Kiploka. et al, *Sensors and Actuators A Physical*, 110, 142 (2004).
- [10] W.Zhang, Y.Li, L.Wie, Y. Fang, *Materials Letters*, 57, 3366 (2003).
- [11] X.Kornman, H. Lindberg, L.A. Berglund., *Polymer*, 42, 1303 (2001).
- [12] J. Madejova; *Vibrational Spectroscopy*, 31(2003) 1-10.
- [13] R.M. Silverstein, F.X. Webster *Spectrometric.* 6th edition (1998) John Wiley, New York.
- [14] D. S. Orlov; *Soil Chemistry*, Oxford/IBH, New Delhi(1992).
- [15] Z. Li, L. Gallus, *Colloids Surf. A* 264, (2005) 61-67.
- [16] Y. Z. Xi, H. He, L. Ding; *J Colloid Interface Sci.* 277(2004) 116-20.
- [17] Q. Zhou, R.L. Frost, H. He, Y. Xi, M. Zbik; *J. Colloid Interface Sci.*, 311(2007) 24-37.